Supplemental Material

(U-Th)/He thermochronology of Grand Canyon resolves 1250 Ma unroofing at the Great Unconformity and <20 Ma canyon carving

Thurston[1], Olivia G., Guenthner[1], William R., Karlstrom[2], Karl E., Ricketts[3], Jason W., Heizler[4], Matthew T., and Timmons[4], J. Michael

[1]University of Illinois at Urbana-Champaign, Urbana, IL
[2]University of New Mexico, Albuquerque, NM, 87106
[3]University of Texas at El Paso, El Paso TX
[4]New Mexico Bureau of Geology and Mineral Resources, NM Tech, Socorro, NM

<u>Contents:</u>
Methods
Forward Models
Inverse Model Geologic Constraints
Supplemental References Cited

Methods:

Zircon separates were used from prior U-Pb geochronology and Hf studies (Holland et al., 2018) which applied standard separation procedures. Four to seven single-grain aliquots from each sample (Fig. S1A) were selected for (U-Th)/He analysis performed at the University of Illinois at Urbana-Champaign (UIUC) utilizing the Ault et al. (2018) method to exploit the full range of radiation damage present in each sample. This selection process relies upon the degree of opacity as a proxy for radiation damage (and eU concentration), where clear grains suggest low damage and fully opaque grains suggest high damage. (U-Th)/He analytical methods followed those described in Guenthner et al. (2016). Helium extraction and analysis consisted of *in vacuo* diode laser heating; cryogenic purification; and quadrupole mass-spectrometry on a Pfeiffer PrismaPlus. U and Th analyses by isotope dilution were completed at UIUC using a Thermo iCAP-Q inductively coupled plasma-mass spectrometry (ICP-

MS), as well as at the University of Arizona using a Thermo Element2 high-resolution ICP-MS. Dimension measurements for zircon were collected for both alpha ejection correction and to calculate eU concentrations. Alpha ejection used the equations of Hourigan et al. (2005).

Forward Models:

Forward models were used to bracket a region of t-T space with end-member scenarios and a few points fixed by independent observations. The models serve to illustrate the sensitivity of a date-eU curve to different aspects of the thermal history and not to determine best fit. They address two related questions: what are the key t-T segments that have the most leverage in shaping a date-eU curve versus what t-T segments are the date-eU curves insensitive to? We used a Matlab script presented in Guenthner (2021) for our forward models, which take time-temperature (t-T) paths as inputs and return modeled date-eU correlations as output. These tests focus on the characteristics of the 1.7 Ga thermal history that have the greatest influence on the shape of the date-eU curves for our samples.

Figure S1A examines the effects of single basement cooling events where basement was exhumed from mid-crustal temperatures (500 °C) to near surface temperatures (20 °C) during different discrete Precambrian episodes: 1350-1250 Ma (pre-Unkar), 1050-950 Ma (post-diabase), or 700-600 Ma (snowball Earth). Grain size effects are shown as envelopes color-coded to each episode. Samples are grouped according to their location: in eastern Grand Canyon (red= Upper Granite Gorge, from river mile 79 to 99), central Grand Canyon (blue= Middle Granite Gorge from river mile 115 to 132, including both the 1.84 Ga Elves Chasm Gneiss and a 1.1 Ga diabase sample), and western Grand Canyon (black = Lower Granite Gorge at river mile 236).

These curves generally fit our data but are not especially discriminating. Model output curves for a 1350-1250 Ma cooling episode pass through more of the Eastern Grand Canyon dates between ~300 and ~100 Ma than a 700-600 Ma cooling pulse, which has a date-eU correlation shifted to eU concentrations too high to match the majority of the observed dates. The post-diabase cooling curve passes through the same region of date-eU space as the five diabase aliquots. Figure S1B tests peak temperatures reached at the end of the Mesozoic (80 Ma) due to slow burial by Devonian to Cretaceous strata; these data suggest that peak late Mesozoic burial temperatures between 140 and 160 °C capture more of the observed data than higher or lower temperature reheating events, in general agreement with (but ~20 °C hotter than) estimates from AHe and AFT thermal history models (Karlstrom et al., 2020, their Fig. 15) and showing that

reheating of 180 °C would have fully reset zircon He dates. Superimposed on the better paths from DR-1A (pre-Unkar) and DR-1B (160 °C reheating), Figure S1C explores the thermal effects of potential ~75 °C variations (black curves) caused by deposition and erosion of the ~ 2-km-thick Unkar and Chuar group basins and suggests that formation of these basins does not have a fundamental effect on date-eU model output as the two date-eU envelopes perfectly overlap. Figure S1D tests thermal histories that correspond to three canyon incision models: "old" (70-60 Ma), "intermediate" (20-0 Ma), and "young" (6-0 Ma) cooling (c.f. Flowers and Farley, 2012; 2013 Karlstrom et al., 2014; 2020) and shows that the "old" canyon model cannot explain the 3-23 Ma dates.

Inverse Model Geologic Constraints:

This section describes in detail the various constraints used to construct our constraint boxes for HeFTy (version 1.9.3, Ketcham, 2005) inverse modeling shown in Figure 3 of the main paper. These are summarized in Table DR-2 and Table DR-3 and elaborated upon below. The bedrock of the Grand Canyon is composed of two major cratonic terranes: the Mojave west of river mile 98 and the Yavapai east of river mile 98. Both provinces yield a high-grade metamorphic age from phase assemblages of 1.70 Ga related to the Yavapai orogeny of Karlstrom et al. (1987) and Karlstrom and Bowring (1988) and the Ivanpah orogeny of Wooden and Miller (1990). Combined, the basement rocks of the Grand Canyon are referred to as the Granite Gorge Metamorphic Suite and the Zoroaster Plutonic Complex, which range in age from 1840 Ma to 1375 Ma and collectively make up the volcanic and sedimentary rocks that formed as a result of the orogenies that sutured together the Mojave and Yavapai provinces (Karlstrom et al., 2012).

Lying unconformably above the Granite Gorge Metamorphic Suite and Zoroaster Plutonic Complex is the Unkar Group, a ~2-km-thick sedimentary sequence deposited between 1254 Ma and 1104 Ma (Timmons et al., 2012). The Unkar Group formed as an inboard foreland basin deposit associated with the Grenville Orogeny and assembly of Rodina (Timmons et al., 2012). The deposition of the 1.1 Ga Cardenas Basalt and diabase feeder dikes marks the end of the Unkar Group and is associated with widespread volcanism in the continental interior. Stratigraphically above the Unkar Group, the Chuar Group is a ~1600-m-thick sedimentary sequence deposited between 775 Ma and 729 Ma (Dehler et al., 2012). The Chuar Group formed in a rift basin associated with the break-up of Rodina (Dehler et al., 2017). The Great Unconformity places different-age sedimentary successions atop unroofed basement. Where Unkar Group was deposited on basement in eastern Grand Canyon this has been

called the Great Nonconformity (Karlstrom et al., 2021) because this surface marks the exhumation of 20-km-deep middle crustal basement rocks to the surface, and hence was the most geologically significant period of basement exhumation. Chuar Group rests with slight angular unconformity atop Unkar Group, but never directly on basement such that deep basement erosion is not documented geologically between 1.1 Ga and 725 Ma. The Cambrian Tonto Group was deposited flat on all prior units producing the Great Angular Unconformity where it rests on tilted Unkar and Chuar strata, and the Great Unconformity (after Dutton, 1882) where is rests on basement (Karlstrom et al., 2021). The overall conclusion from the geology is that there are multiple unconformities that make up the Great Unconformity (Karlstrom and Timmons, 2012); this should be the starting point for any thermochronologic modeling.

Deposition of sedimentary strata dominates the geology of the Grand Canyon in the Paleozoic and Mesozoic eras with accumulation of about 4 km of strata in the region by 80 Ma suggested by both stratigraphic reconstructions (Karlstrom et al., 2017) and apatite thermochronology (see summary in Karlstrom et al., 2020). Rapid cooling associated with the Laramide Orogeny after 80 Ma is recorded in apatite thermal history modeling in many samples (Kelley et al., 2012; Flowers et al., 2008; Flowers and Farley, 2012; Lee et al., 2012; Karlstrom et al., 2014). Additional cooling pulses are recorded 25-15 Ma and post- 6 Ma that are related to multi-stage canyon incision with different histories recorded in different segments of Grand Canyon. Incision of Grand Canyon as we see it today took place in the past 5-6 Ma as the Colorado River became integrated through older paleocanyon segments (Karlstrom et al., 2014) and reached the Gulf of California after 5 Ma (Crow et al., 2021).

Inverse Model Grain Inputs:

Given the large degree of second-order dispersion in our measured dataset (i.e. dispersion not attributable to radiation damage effects alone), we used a synthetic grain approach to inversely model date-eU correlations. An important limitation of HeFTy modeling with ZRDAAM, or any kinetic model, is that the program assumes that all observed date dispersion can be perfectly explained (i.e. no error in kinetics) by the particular kinetic model being used. That is, the goodness-of-fit statistics only assess how well a certain t-T path matches the data inputs for radiation damage-caused dispersion alone. Other important sources of date dispersion, such as U-Th zonation, are not accounted for. In our data, we observe from forward model results (Fig. S1) that, whereas first order date-eU trends are apparent, no single curve can match or explain all of the ZrHe dates. The relative influences of radiation damage versus other

sources of dispersion should therefore guide the motivations of inverse modeling: If date-eU correlations are relatively precise and explain a large percentage of observed dispersion, then inverse models can be used to more narrowly constrain or "find" viable t-T solutions from the measured data. In contrast, if a large degree of non-radiation damage influenced date dispersion is apparent, then inverse modeling should be viewed as only a means to determine how much of the dispersion is due to radiation damage effects, and whether the measured dates conform to previously determined geologic constraints. For our dataset, we use inverse modeling in the latter sense.

Inputs for these synthetic grains (reported as corrected ages) are as follows: 1) 201 ± 159 Ma, 306 ppm, 45 μm, 2) 51.3 ± 45.5 Ma, 595 ppm, 52 μm, and 3) 9.21 ± 7.04 Ma, 1481 ppm, 55 μm. For our AHe and AFT inputs, we selected previously published samples that spanned the same river miles as our eastern Grand Canyon samples (79.6-115), and had results for both apatite thermochronometers: 98GC20 (Fig. S2) and 98GC11 (Kelley et al., 2001; Lee et al., 2013). The AHe data was averaged with inputs of 40.8 ± 16.7 Ma,11 ppm, 37 μm for 98GC11, and 26.4 ± 3.8 Ma, 9 ppm, 39 μm for 98GC20. AFT inputs were 49.4 ± 3.8 Ma (central age, 1σ) and a mean track length of 11.1 ± 1.0 μm (1σ) for 98GC11, and 46.5 ± 4.9 Ma (central age, 1σ) and a mean track length of 11.7 ± 0.8 μm (1σ) for 98GC20.

Figure S2 shows inverse model results in HeFTy when 98GC20 apatite data is used instead of 98GC11 (results shown in Fig. 3, main text). The models show similar results, however using 98GC11 apatite data for the synthetic grains allows for HeFTy to generate both good and acceptable fit paths, while 98GC20 apatite data only good fit paths. In both models, all acceptable paths nearly fill the constraint boxes and show that the ZHe data do not provide strong constraints on the 1250 to 80 Ma parts of the t-T path, but are consistent with the known geology and Ar –Ar and apatite thermochronology in suggesting that the main basement exhumation took place between 1350 and 1250 Ma, and that the basement rocks underwent further cooling during multiple cooling/ canyon carving events in the Cenozoic: 80-50 Ma, 25-15 Ma, and post-6 Ma.

Table S1: (U-Th)/He zircon data from the basement rocks of the Grand Canyon.

Table S2: Geologic and thermochronologic constraints used in HeFTy inverse models.

Table *S3*: Inputs, settings, and data treatment for thermal history models.

Figure S1: *Forward ZHe models test sensitivity of date-eU relationships (left panels) color coded to different hypothetical t-T paths (right panels). The base t-T path (yellow) for all models is: 1700-1350 Ma at 500 °C, 1350-1250 Ma cooling to 20 °C, 1250-540 Ma at 20 °C, 540-310 Ma heating to 40 °C, 310-80 Ma heating to 140 °C, 80-7 Ma at 140 °C, 7-0 Ma cooling to the surface. Alternative models are shown in other colors and are tested relative to the base model. Solid date-eU curves are for the mean grain size for the entire data set; corresponding envelopes show 1 standard deviation grain size. Major conclusions are: A. Timing of late Proterozoic cooling affects the amount of radiation damage in-growth in each crystal, the maximum age preserved, and the inflection from a positive to a negative correlation between date and eU. B. Timing and maximum temperature of end-Mesozoic reheating affects the extent to which the radiation damaged crystals are reset or completely annealed and is a strong control on the age of inflection and the slope of the negative date-eU curve. C. thermal effects of potential ~100 °C variations (black curves) caused by deposition and erosion of the <4 km thick Unkar plus Chuar group basins do not markedly leverage the ZHe distribution and does not have a fundamental effect on date-eU model; D. Timing of canyon incision (old vs. intermediate vs. young) markedly influences ages at the highest eU concentrations. Overall, these forward models suggest that the early and late components of ot the t-T history have strongest leverage on the date-Eu distribution and that our ZHe data alone may be relatively insensitive to minor heating and cooling due to late Proterozoic basins and unroofing events.*

Figure S2: *HeFTy inverse model results for the Eastern Grand Canyon using synthetic ZHe dates (see text) and AHe and AFT data from 98GC20 as inputs. Labels next to each constraint box (a-p) in panel A correspond to constraints described in table DR-2. Results are consistent with geologic data that indicate a major period of basement cooling from 250 to <100 °C during exhumation of middle crustal rocks to the surface before Unkar Group deposition at 1.25 Ga. Late-stage rapid cooling post-20 Ma to 50 °C, and cooling from 50 °C to surface after ~ 10 Ma.*

References Cited:

Ault, A.K., Guenthner, W.R., Moser, A.C., Miller, G.H. and Refsnider, K.A., 2018. Zircon grain selection reveals (de) coupled metamictization, radiation damage, and He diffusivity. *Chemical Geology*, *490*, pp.1-12.

Blakey, R.C. and Middleton, L.T., 2012. Geologic history and paleogeography of Paleozoic and early Mesozoic sedimentary rocks, eastern Grand Canyon, Arizona. Spec. Pap., Geol. Soc. Am, 489, pp.81-92.

Conway, C.M. and Silver, L.T., 1989. Early Proterozoic rocks (1710–1615 Ma) in central to southeastern Arizona. Arizona Geological Society Digest, 17, pp.165-186.

Crow, R., Schwing, J., Karlstrom, K.E., Heizler, M., Pearthree, P., House, P.K., Dulin, S., Janeke, S.U., Stelten, M., and Crossey, L.J., 2021, Refining the age of the Colorado River: Geology, v. 49., https://doi.org/10.1130/G48080.1

Dehler, C.M., Porter, S.M., Timmons, J.M. and Karlstrom, K.E., 2012. The Neoproterozoic Earth system revealed from the Chuar Group of Grand Canyon. Grand Canyon Geology: Two Billion Years of Earth's History: Geological Society of America Special Paper, 489, pp.49-72.

Dehler, C., Gehrels, G., Porter, S., Heizler, M., Karlstrom, K., Cox, G., Crossey, L. and Timmons, M., 2017. Synthesis of the 780–740 Ma Chuar, Uinta Mountain, and Pahrump (ChUMP) groups, western USA: Implications for Laurentia-wide cratonic marine basins. Bulletin, 129(5-6), pp.607-624.

DeLucia, M.S., Guenthner, W.R., Marshak, S., Thomson, S.N. and Ault, A.K., 2018. Thermochronology links denudation of the Great Unconformity surface to the supercontinent cycle and snowball Earth. Geology, 46(2), pp.167-170.

Dumond, G., Mahan, K.H., Williams, M.L. and Karlstrom, K.E., 2007. Crustal segmentation, composite looping pressure-temperature paths, and magma-enhanced metamorphic field gradients: Upper Granite Gorge, Grand Canyon, USA. Geological Society of America Bulletin, 119(1-2), pp.202-220.

Dutton, C.E., 1882, Tertiary History of the Grand Canon District; with atlas: Department of the Interior, Monographs of the United States Geological Survey, Volume II: 263 p.

Flowers, R.M. and Farley, K.A., 2012. Apatite 4He/3He and (U-Th)/He evidence for an ancient Grand Canyon. Science, 338(6114), pp.1616-1619.

Flowers, R.M. and Farley, K.A., 2013. Response to comments on "Apatite 4He/3He and (U-Th)/He evidence for an ancient Grand Canyon". Science, 340(6129), pp.143-143.

Flowers, R.M., Wernicke, B.P. and Farley, K.A., 2008. Unroofing, incision, and uplift history of the southwestern Colorado Plateau from apatite (U-Th)/He thermochronometry. Geological Society of America Bulletin, 120(5-6), pp.571-587.

Guenthner, W.R., Reiners, P.W. and Chowdhury, U., 2016. Isotope dilution analysis of Ca and Zr in apatite and zircon (U-Th)/He chronometry. Geochemistry, Geophysics, Geosystems, 17(5), pp.1623-1640.

Guenthner, W.R., 2021. Implementation of an alpha damage annealing model for zircon (U-Th)/He thermochronology with comparison to a zircon fission track annealing model. Geochemistry, Geophysics, Geosystems, 22(2), p.e2019GC008757.

Hourigan, J.K., Reiners, P.W. and Brandon, M.T., 2005. U-Th zonation-dependent alpha-ejection in (U-Th)/He chronometry. Geochimica et Cosmochimica Acta, 69(13), pp.3349-3365.

Ketcham, R. A., 2005. Forward and inverse modeling of low-temperature thermochronometry data, in Low-Temperature Thermochronology: Techniques, Interpretations, and Applications, edited by P. W. Reiners and T. A. Ehlers, Mineral. Soc. Am. Rev. Min. Geochem., 58, 275–314.

Karlstrom, K.E., Bowring, S.A. and Conway, C.M., 1987. Tectonic significance of an Early Proterozoic two-province boundary in central Arizona. Geological Society of America Bulletin, 99(4), pp.529-538.

Karlstrom, K.E. and Bowring, S.A., 1988. Early Proterozoic assembly of tectonostratigraphic terranes in southwestern North America. The Journal of Geology, 96(5), pp.561-576.

Karlstrom, K.E., Ilg, B.R., Williams, M.L., Hawkins, D.P., Bowring, S.A., and Seaman, S.J., 2003. Paleoproterozoic rocks of the Granite Gorges, in Beus, S.S. and Morales, M., eds., Grand Canyon Geology: Oxford University Press, second edition, p. 9-38.

Karlstrom, K.E. and Timmons, J.M., 2012. Many unconformities make one 'Great Unconformity'. Grand Canyon Geology; Two Billion Years of Earth's History, pp.73-79.

Karlstrom, K.E., Lee, J.P., Kelley, S.A., Crow, R.S., Crossey, L.J., Young, R.A., Lazear, G., Beard, L.S., Ricketts, J.W., Fox, M. and Shuster, D.L., 2014. Formation of the Grand Canyon 5 to 6 million years ago through integration of older palaeocanyons. Nature Geoscience, 7(3), pp.239-244.

Karlstrom, K.E., Crossey, L.J., Embid, E., Crow, R., Heizler, M., Hereford, R., Beard, L.S., Ricketts, J.W., Cather, S., Kelley, S., 2017, Cenozoic incision history of the Little Colorado River: its role in carving Grand Canyon and onset of rapid incision in the last ~2 Ma in the Colorado River System: Geosphere CRevolution volume, v. 13, no. 1, p. 49-81 doi:10.1130/GES01304.1.

Karlstrom, K.E., Jacobson, C.A., Sundell, K.E., Eyster, A., Blakey, R., Ingersoll, R.V., Mulder, J.A., Young, R.A., Beard, L.S., Holland, M.E., Shuster, D.L., Winn, C., and Crossey, L.J., 2020, Evaluating the Shinumo-Sespe drainage connection: Arguments against the "old" (70–17 Ma) Grand Canyon models for Colorado Plateau drainage evolution: Geosphere, v. 16, https://doi.org/10.1130/GES02265.1.

Karlstrom, K.E., Mohr, M.T., Schmitz, M.D., Sundberg, F.A., Rowland, S.M., Blakey, R., Foster, J.R., Crossey, L.J., Dehler, C.M. and Hagadorn, J.W., 2020. Redefining the Tonto Group of Grand Canyon and recalibrating the Cambrian time scale. Geology, 48(5), pp.425-430.

Karlstrom, K., L. Crossey, A. Mathis, and C. Bowman. 2021. Telling time at Grand Canyon National Park: 2020 update. Natural Resource Report NPS/GRCA/NRR—2021/2246. National Park Service, Fort Collins, Colorado. https://doi.org/10.36967/nrr-2285173.

Kelley, S.A., Karlstrom, K.E. and Timmons, J.M., 2012. The Laramide and post-Laramide uplift and erosional history of the eastern Grand Canyon: Evidence from apatite fission-track thermochronology. Grand Canyon geology: Two billion years of Earth's history: Geological Society of America Special Paper, 489, pp.109-117.

Lee, J.P., Stockli, D.F., Kelley, S.A., Pederson, J.L., Karlstrom, K.E., and Ehlers, T.A., 2013, New thermochronometric constraints on the Tertiary landscape evolution of central and eastern Grand Canyon, Arizona: Geosphere, v. 9, no. 2, p. 216–228, doi: 10 .1130 /GES00842 .1
.Timmons, J.M. and Karlstrom, K.E. eds., 2012. Grand Canyon Geology:

Two Billion Years of Earth's History (Vol. 489). Geological Society of America.

Wooden, J.L. and Miller, D.M., 1990. Chronologic and isotopic framework for Early Proterozoic crustal evolution in the eastern Mojave Desert region, SE California. Journal of Geophysical Research: Solid Earth, 95(B12), pp.20133-20146.Special Paper, 489, pp.109-117.

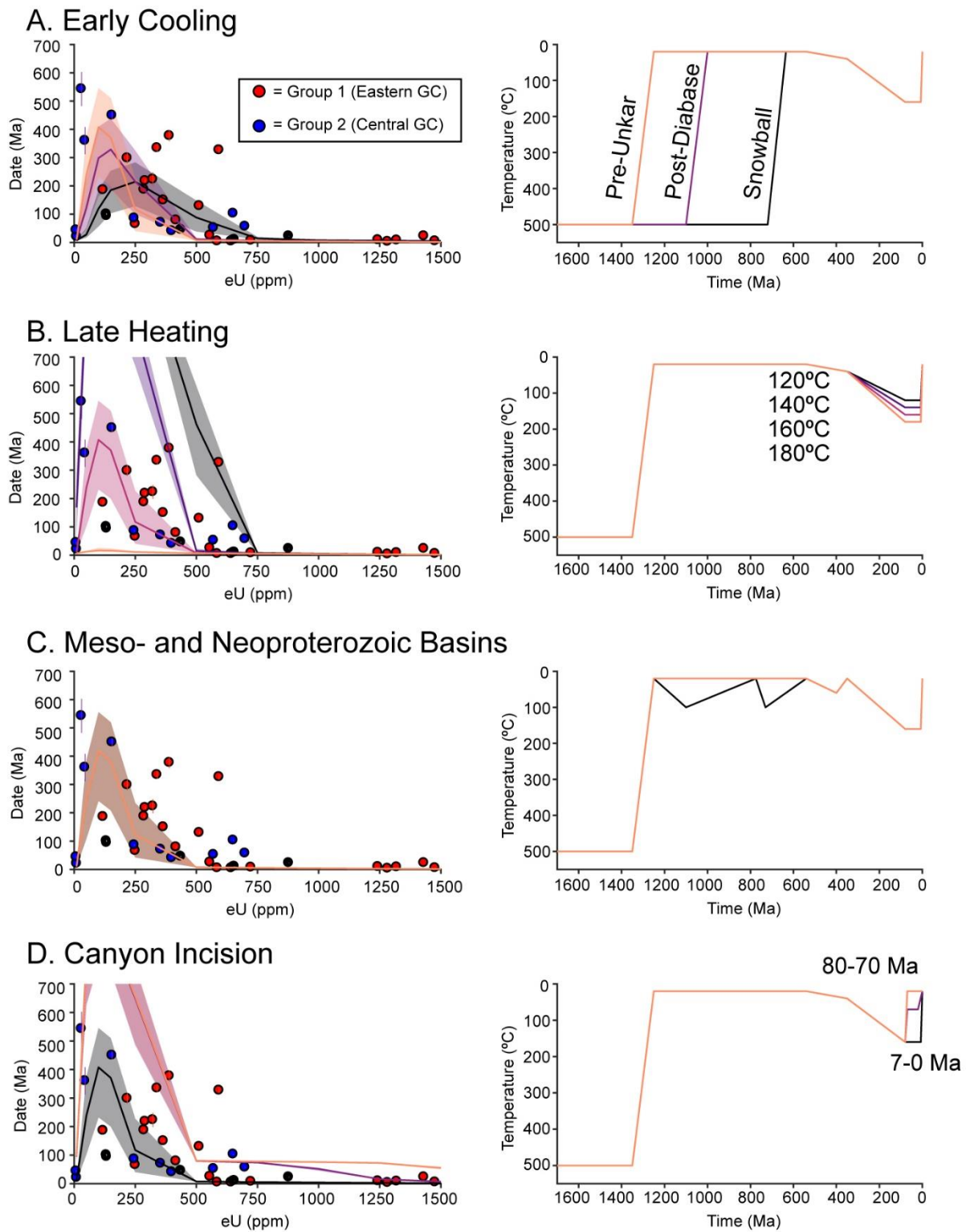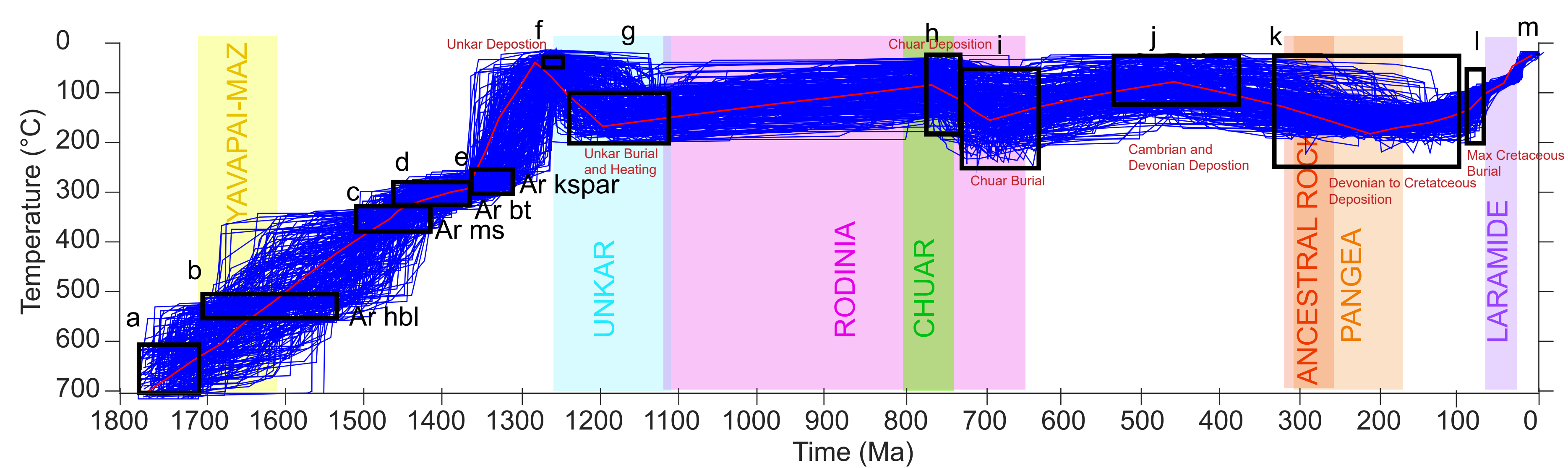Figure S1

Figure S2